



Influence of Large-scale PV on Voltage Stability of Sub-transmission System

Rakibuzzaman Shah¹, Nadarajah Mithulananathan¹, Ramesh Bansal¹,
Kwang Y. Lee² and Abraham Lomi³

¹The school of Information Technology and Electrical Engineering,
The University of Queensland, Brisbane, QLD-4072, Australia

²Department of Electrical and Computer Engineering, Baylor University, Waco, Tx 76798-7356, USA

³Department of Electrical Engineering, Institut Teknologi Nasional, Malang, Indonesia

Abstract: Voltage instability is considered as one of the main threats to secure operation of power systems around the world. Grid connected renewable energy-based generation are deploying in recent years for many economic and environmental reasons. This type of generation could have significant impact on power system voltage stability given the nature of the primary source for generation and the technology used for energy conversion. This paper presents the results of an investigation of static voltage stability in heavily stressed IEEE-14 bus test system with large-scale PV integration. The study focused on the impact of large-scale PV penetrations and dynamic VAR placements on voltage stability of the sub-transmission system. For this study, the test system loads are modeled as the summer peak load of a realistic system. The comparison of STATCOM and SVC performance with large-scale PV is also discussed.

Keywords: PV generator, STATCOM, SVC, trajectory sensitivity index, voltage stability.

1. Introduction

Utilization of renewable energy comes from the perspective of environmental conservation and fossil fuel shortage. Recent studies suggest that in medium and long terms, photovoltaic (PV) generator will become commercially so attractive that large-scale implementation of this type can be seen in many parts of the world [1], [2]. A large-scale PV generation system includes photovoltaic array, maximum power point tracking (MPPT), DC/AC converter and the associated controllers. It is a multivariable and non-linear system, and its performance depends on environmental conditions. Recently, the increasing penetration levels of PV plants are raising concerns to utilities due to possible negative impacts on power system stability as speculated by a number of studies [3]-[5]. Thus, the thorough investigation of power system stability with large-scale PV is an urgent task.

Among stability issues, voltage instability has been a major concern for power system. Several major power interruptions have been linked to power system voltage instability in recent past [6], [7]. It has been proved that inadequate reactive power compensation during stressed operating condition can lead to voltage instability. Although large-scale PV is capable of generating reactive power, however, the operation of PV in terminal voltage mode has the potential for adverse interaction with other voltage controllers [8]. Therefore, grid code requires operation at power factors equal or greater than 0.95 for PV generators [9], [10]. Moreover, the size and position of large-scale PV generator can introduce detrimental effect on power system voltage stability as the level of PV penetration increased.

Furthermore, the technical regulations or specific standards are trying to shape the conventional control strategies to allow the flawless integration of renewable energy based distributed generation (DG) in main grid. According to technical regulations or standards the post fault voltage recovery time at DG bus is crucial as it requires DG to trip, if recovery time exceeds certain limits [9], [10]. With increased penetration of renewable energy DG, early

tripping of DG due to local disturbance can further risk the stability of the system. Hence system operator becomes responsible to maintain the voltage profile under all operating conditions. As a result, fault tolerant control algorithm based on dynamic VAR planning (e.g. placement of FACTS) is applied in DG integrated system. The most common, or preferred, dynamic VAR planning with multiple DGs is the placement of dynamic VAR device at the point of common coupling of DG.

In this paper, the result of static voltage stability with large-scale PV penetrations on sub-transmission system for realistic load composition is presented. Three dynamic VAR placements algorithms are compared in terms of long-term voltage stability with large-scale PV penetrations. The impact of SVC and STATCOM placement on static voltage stability is studied, and their performances are compared.

The rest of the paper is organised as follows. Section II presents the methodologies used for static voltage stability analysis followed by the underlying concept of trajectory sensitivity index. Modelling of PV and dynamic VAR compensators are illustrated in Section III. Section IV briefly introduces the test system and its composition. Study results based on IEEE-14 bus test system are presented in Section V. Section VI gives the relevant conclusions.

2. Methodology

A. Q-V Modal Analysis

The analytical description of a power system applicable to stability study is given by the following differential-algebraic equation [11]

$$\dot{x} = f(x, y, \lambda) \quad (1)$$

$$0 = g(x, y, \lambda) \quad (2)$$

where, $x \in \mathfrak{R}^n$ is a vector of state variables; $y \in \mathfrak{R}^m$ is a vector of algebraic variables (e.g., load voltage phasor magnitude and angles); $\lambda \in \mathfrak{R}^l$ is a set of uncontrollable phasor magnitude such as variation of active and reactive power of loads. The set of system algebraic equations can be expressed as follows:

$$\begin{bmatrix} \Delta P \\ \Delta Q \end{bmatrix} = \begin{bmatrix} \frac{\partial P}{\partial \theta} & \frac{\partial P}{\partial V} \\ \frac{\partial Q}{\partial \theta} & \frac{\partial Q}{\partial V} \end{bmatrix} \begin{bmatrix} \Delta \theta \\ \Delta V \end{bmatrix} \quad (3)$$

where, ΔP , ΔQ are mismatch power vectors. ΔV , $\Delta \theta$ are unknown voltage magnitude and angle correction vectors.

For steady state voltage stability analysis, the change of active power is considered as constant (zero) in power flow Jacobian. After some manipulation, from eq. (3) we can get the reduced Jacobian (J_R) as

$$J_R = \xi_{n \times n} \Lambda_{n \times n} \eta_{n \times n} \quad (4)$$

where, ξ = matrix of right eigenvectors corresponding to all eigenvalue of the system, Λ = diagonal matrix of system eigenvalues and η = matrix of left eigenvectors corresponding to all eigenvalues of the system. By using (4) expression for modal voltage and modal reactive power variations corresponding to i^{th} eigenvalue can be obtained,

$$v_i = \lambda_i^{-1} q_i \quad (5)$$

where, v_i = modal voltage variation and q_i = modal reactive power variation, λ_i = eigenvalue of i^{th} mode obtained from J_R system matrix.

Magnitude and sign of λ_i (Q-V modal eigenvalue) provides the information of system static voltage stability. As the system becomes stressed, one of the eigenvalues of J_R becomes smaller and the modal voltage becomes weaker. If the magnitude of the eigenvalue is equal to zero, the corresponding modal voltage is at the point of collapse. A system is called as voltage stable if all the eigenvalues of J_R matrix are positive, if any of the eigenvalue is negative, the system is unstable [11].

B. Continuation Power Flow

Continuation power flow solution allows the solutions of multiple power flows to be found from a given starting point to the critical point. The stability information that can be obtained by the continuation power flow is typically associated with system loading margin. Algebraic equations of the system are taken into account for continuation power flow evaluation. For continuation power flow analysis, analytical description of a power system can be described as

$$0 = g(y, \lambda) \quad (6)$$

In continuation power flow analysis, PV generators are modeled as PQ or PV generator with reactive power limits as mentioned in [12].

C. Trajectory Sensitivity Index

From DAE of power system, the flows of x and y can be defined as [13]:

$$x(t) = \psi_x(x_0, t, \lambda) \quad (7)$$

$$y(t) = \psi_y(x_0, t, \lambda) \quad (8)$$

Sensitivities of system flow regarding initial conditions and parameters are obtained by a Taylor's series expansion of (7) and (8):

$$\Delta x(t) = \frac{\partial x(t)}{\partial \lambda} \Delta \lambda = x_\lambda(t) \Delta \lambda \quad (9)$$

$$\Delta y(t) = \frac{\partial y(t)}{\partial \lambda} \Delta \lambda = y_\lambda(t) \Delta \lambda \quad (10)$$

The sensitivities of x_λ and y_λ can be evaluated along the trajectory, known as trajectory sensitivities. Simple numerical procedure can be used to obtain these sensitivities from non-linear simulations (time domain simulations):

$$x_\lambda = \frac{\psi_x(x_0, t, \lambda + \Delta \lambda) - \psi_x(x_0, t, \lambda)}{\Delta \lambda} \quad (11)$$

$$y_\lambda = \frac{\psi_y(x_0, t, \lambda + \Delta \lambda) - \psi_y(x_0, t, \lambda)}{\Delta \lambda} \quad (12)$$

In this paper, the trajectory sensitivities are used to decide the suitable placement of dynamic VAR device such as STATCOM for fast voltage recovery of multiple PV generators in the

system. Sensitivity of i^{th} bus voltage (V) with respect to reactive power (Q) injection at j^{th} bus can be calculated as $\frac{\partial v_i}{\partial Q_j}$. Then the trajectory sensitivity index proposed in [15] is defined as

$$TSI_j = \sum_{k=1}^{N_k} w_k \left[\sum_{i=1}^n w_{bi} \left[\frac{\partial v_i}{\partial Q_j} \right]_{t=t_k} \right] \quad (13)$$

where, w_{bi} is the weighting factor to represent the importance of i^{th} bus on the sensitivity and w_{bi} has been chosen to be 1 for all the load buses and the buses with PV generators. w_k is the weighting factor to designate the importance of time instant k . Higher value of w_k is selected for the time instants just after the fault. Bus with higher trajectory sensitivity index is the the best location for dynamic VAR placement with multiple PVs.

3. PV Generator and Dynamic Var Compensator Modelling Overview

A. PV Generator Modelling Overview

For large-scale operation of PV, modules are connected in series and parallel to form an array. The array output current equation can be derived from the basic solar cell output current equation and can be expressed as [16]

$$I_{PV} = I_{SCA}(G) - N_P \times I_0 \left[e^{\frac{(V_A + I_{PV} R_s)q}{nN_S kT}} - 1 \right] \quad (14)$$

where, I_{PV} = array current (A), V_A = array voltage (V), q = electron charge ($1.6 \times 10^{-19} \text{ C}$), k = Boltzmann's constant (1.38×10^{-19}), n = ideal factor, T = ambient temperature, I_0 = diode reverse saturation current (A), R_s = array series resistance (Ω), $I_{SCA}(G) = N_p I_{SC}(G)$, $N_S = N_{CS} N_{SM}$, $N_P = N_{SP}$, N_{SM} and N_{SP} represent the number of modules connected in series and parallel in the photovoltaic array, respectively, N_{CS} = number of series connected cells in a module, I_{SC} = cell short circuit current (A) and G = solar insolation at any instant (W/m^2).

DC power generated from PV array is considered to be the real power injected into the network. Real and reactive power generation from the PV system is controlled by voltage source converter. For proper analysis, three-phase inverter terminal voltage is converted into d-q axis voltage component (Park's voltages). Park's voltages are related to the PV array terminal voltage by following relationship [17]:

$$\begin{cases} V_d = \frac{\sqrt{3}mV_A}{2\sqrt{2}} \cos \delta \\ V_q = -\frac{\sqrt{3}mV_A}{2\sqrt{2}} \sin \delta \end{cases} \quad (15)$$

where, m is modulation index (0,1), δ is the phase angle ($\pm\pi/2, 0$) and V_A represents PV array terminal voltage. Let us assume that the DC power generated by the PV array is delivered to the network, then

$$P_{dc} = P_{ac} = \frac{0.6128 m V_A V_s \sin \delta}{X_t} \quad (16)$$

and, the reactive power equation of the PV generator can be represented as

$$Q_{ac} = \frac{0.6128 mV_A \cos \delta}{X_t} - \frac{V_s}{X_t} \quad (17)$$

where, V_s = grid bus voltage (V), and X_t = impedance between inverter terminal and grid bus (Ω).

B. Statcom Model

STATCOM is a voltage source converter (VSC) based system that injects or absorbs reactive current, independent to grid voltage. Basic structure and terminal characteristic of STATCOM is shown Figure 1 [18]. The STATCOM current is always kept in quadrature in relation to the bus voltage so that only reactive power is exchanged in between AC system and STATCOM bus. The current injected by STATCOM depends on pulse width modulation (PWM) method used along with operational limits and characteristics of Insulated Gate Bipolar Transistors (IGBTs) in use. Hence, current injected by STATCOM has appropriate limits, which are dynamic in nature [19].

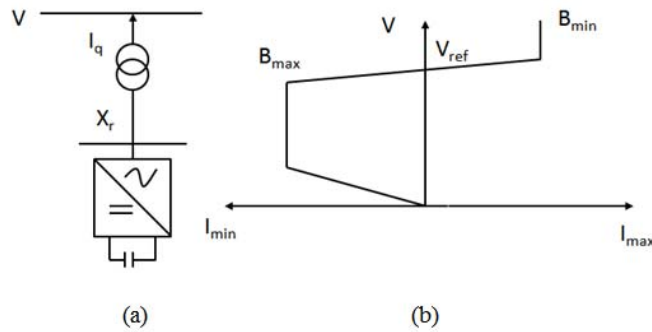


Figure 1. (a) Basic Structure of STATCOM, (b) terminal characteristic of STATCOM.

C. SVC Model

Static VAR Compensator (SVC) is the most extensively used dynamic VAR compensator whose output is adjusted to exchange capacitive and inductive current so as to maintain or control specific system variables, the bus voltage. For maximum or minimum susceptance limit, SVC behaves like a fixed capacitor or an inductor. Figure 2 shows the basic structure and terminal characteristic of a SVC [18].

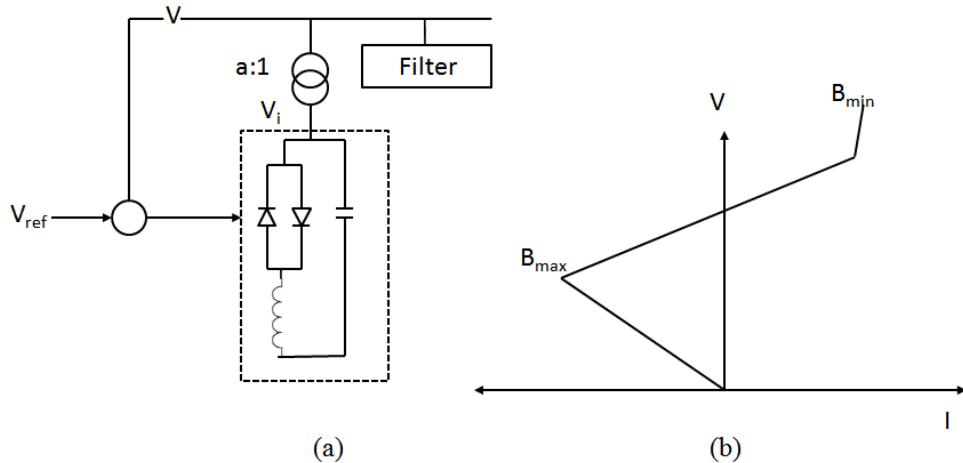


Figure 2. (a) Basic structure of SVC, (b) terminal characteristic of SVC.

4. Test System and its Composition

A. Test System

On-line diagram of IEEE-14 bus test system is depicted in Figure 3. In original test system, there are five synchronous generators among which three of them are synchronous compensators used only for reactive power support, and two generators are located at buses 1 and 2 [18]. There are twenty branches and fourteen buses with eleven load buses. For this study, a slightly modified IEEE-14 bus system is considered. The modification from original IEEE-14 bus system is that generators located at buses 3 and 6 are changed from synchronous compensators to synchronous generators and the loading of the system are increased to 362.5 MW and 108.5 MVar, respectively. Results included in this paper are obtained by using MATLAB and MATLAB based power system analysis software known as PSAT [20].

B. Load Composition

Proper modelling of loads for power system static voltage stability study is important as they have profound impact on voltage stability. Utilities break their loads into various compositions with presence of different percentages of loads. For this study, loads are modeled as the summer peak load of a realistic system. The active part of the load is modeled as 100 % constant current and reactive part of the load is modeled as 100 % constant impedance load [21].

PV Generation and It Size

An aggregated PV generator depicted in Figure 4 is used for the analysis. A 10 MVA PV generator is considered for the initial analysis; while for the investigation of the penetration effect of PV on static voltage stability, PV generator size is increased by 10 MVA step size. Aggregated PV generator data are taken from [12].

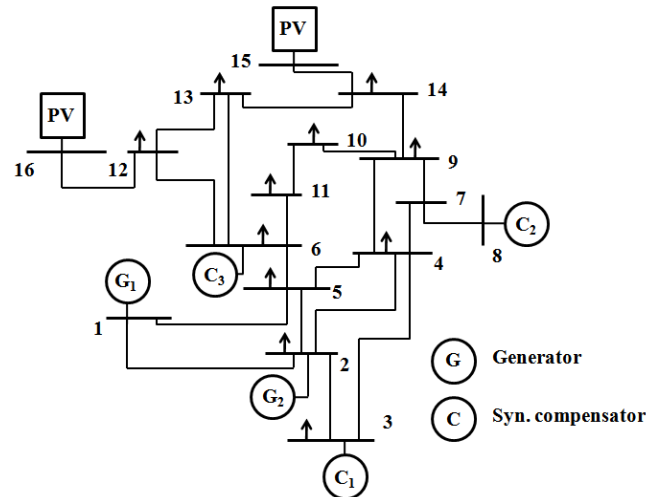


Figure 3. Single-line diagram of IEEE-14 bus test system.

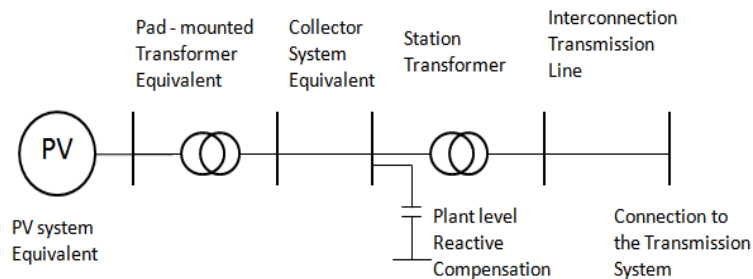


Figure 4. Schematic diagram of an aggregated PV generator.

5. Results and Analysis

A. Effect of PV Penetration on Static Voltage Stability

First, Q-V modal analysis has been performed for the system with and without PV. Table I summarises the critical eigenvalue of the system with and without PV. PV generator is integrated at the midpoint in between bus 14 and 9 of the test system. The analysis has been carried out with constant power factor (0.95 lead-lags) and voltage control mode operation of PV. Results in Table I indicate that integration of PV to the system with constant power factor operation reduces the degree of system voltage stability (from 2.6855 to 1.5706). However, if the same integrated PV operates at voltage control mode, degree of system voltage stability improves (from 2.6855 to 3.6155).

Table 1. Critical Eigenvalue

Mode	Eigenvalue of the system with PV		Eigenvalue of the system without PV
	Power factor operation	Voltage control mode operation	
Most critical mode	1.5706	3.6155	2.6855

Integration of PV generator to the grid depends on various factors like solar insolation; land availability, transmission line right-of-way, etc. So, it may not be possible to integrate the PV generator at the weakest bus or the weak area of the system. However, the loading of the system is not constant at all time. Therefore, the effect of load increase and PV location on system voltage stability has been analyzed next. Normally, for static voltage stability analysis load at each bus is increased at the same rate, referred as conventional loading direction in this paper. But in reality load at different bus can be changed in different direction, for any instant load of some buses may increase while load in other buses remain unchanged or decreased. For this study we have considered both the conventional loading direction and realistic loading direction proposed in [6] to find the loading margin of the system with PV generator. For realistic load direction, IEEE-14 bus system is split into two areas, namely area-1 and area-2. Buses 1-3, 5 and 6 are in area-1 and buses 4, 7-14 are in area-2. Table II summarizes the percentage of load increase and the area factor for realistic loading direction. For this analysis, PVs are placed at different system buses based on bus weakness. An aggregated PV of 10 MVA rating is considered for the analysis. Figure 5 shows the system loading margin for two different loading directions and PV generator locations. From the figure it can be seen that PV locations and loading directions have significant effect on system loading margin. From the results shown in Figure 5 it is worthwhile to note that for conventional and realistic loading direction, system loading margins with power factor operated PV are less than the base case (without PV). However, system loading margins are improved from the base case with the integration of voltage control mode operated PV for both loading directions. It is interesting to note that the realistic loading direction provides lower loading margin than the conventional one at base case, and with PV generator.

Table 2. The Percent of Load Increase and Area Factor for Realistic Loading Direction

Area	% load change	Area factor
1	20.00	0.2944
2	80.00	1.0000

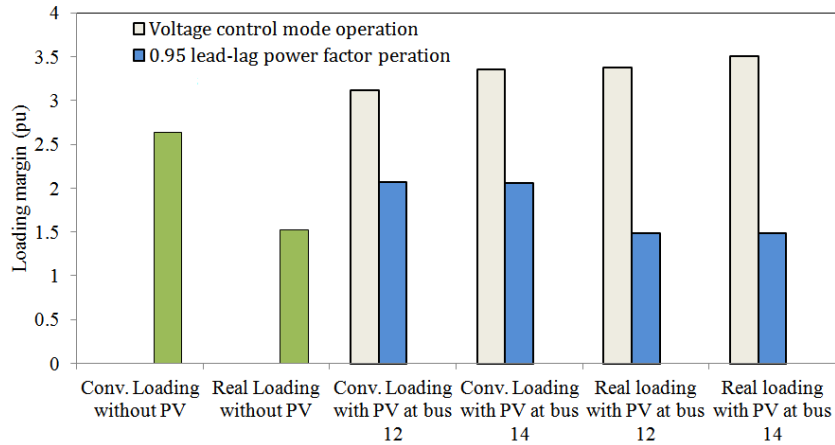


Figure 5. Loading margins for different loading directions (with and without PV).

In case of contingencies, the system characteristics have changed. Effect of PV generator penetration on system voltage stability during contingency is analyzed by the outage of line **1-5**. Table III illustrates the effect of PV locations on system critical eigenvalue for normal and N-1 contingency. Critical eigenvalue of the system at the base case for this particular N-1 contingency is **2.5658**. From Table III it can be observed that for all PV locations critical eigenvalue of the system is higher than the base case at normal operating condition, while during N-1 contingency degree of stability is less than the base case for voltage control mode operated PV at bus 12. From the table it is also noticeable that for all PV locations critical eigenvalue of the system for normal and N-1 contingency is lower than the system base case when integrated PV operated at power factor control mode. From the table, it is worthwhile to note that for voltage control mode operation in most of the cases dispersed PV location improves the degree of voltage stability.

Table 3. Impact of PV Locations on Critical Eigenvalue

PV location bus	Critical eigenvalue (Voltage control mode operation of PV)		Critical eigenvalue (Power factor operation of PV)	
	Normal	N-1 contingency	Normal	N-1 contingency
12	2.6697	2.4025	1.5756	1.5669
13	2.6898	2.6091	2.2618	2.2516
14	3.9398	3.6791	2.3525	2.3315
10,12	4.5266	4.4966	1.775	1.7572
9,13	6.4356	6.4346	1.8595	1.8376
5,14	3.9046	3.8876	1.5683	1.555

B. Effect of PV Penetration

To study the impact of increased PV penetration on voltage stability, the following scenarios are considered,

1. Concentrated PV penetration.
2. Dispersed PV penetration.

Figure 6 shows the effect of concentrated PV penetration on the degree of system stability. From the figure it can be seen that for all the buses increased PV penetration does not have positive impact on system stability. At some location (**e.g., bus 12**), penetration of PV does not appear to contribute to the voltage stability of the system; meanwhile other position (**bus 9**) has both positive and negative impact on voltage stability with incremental penetration. It can be

noted that at bus 9, size up to 20 MVA improves the degree of voltage stability, and beyond 20 MVA the degree of voltage stability has been reduced.

Figure 7 shows the impact of dispersed PV penetration on the degree of system stability. For this study PV generators are placed as follows:

1. All PVs are in the weak area of the system.
2. All PVs are in the strong area of the system.
3. PV penetrations at weak and strong area of the system.

From the figure it can be observed that dispersed PV penetration at buses 4 and 5 enhanced the degree of stability. Whereas, degree of stability is reduced for PV penetration at buses 10 and 14. Degree of system stability remains almost same as base case for PV penetration at buses 5 and 14. Thus, it is worthwhile to mention that for dispersed PV penetration, the degree of stability enhancement strongly depends on the locations of PV.

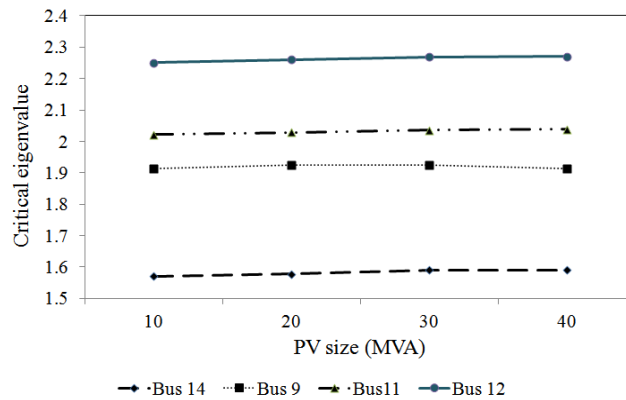


Figure 6. Effect of concentrated PV penetration on the degree of stability

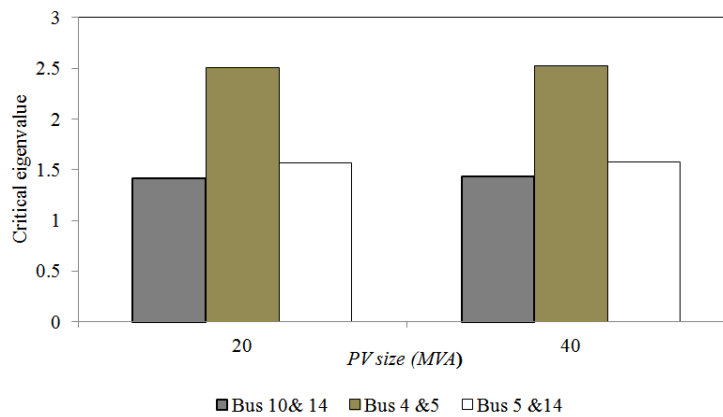


Figure 7. Effect of dispersed PV penetration on the degree of stability.

System loading margins for concentrated and dispersed PV penetrations are depicted in Figure 8. From Figure 8 it is noticeable that concentrated PV penetrations provide higher loading margin than the dispersed PV penetrations for almost all penetration scenarios, except dispersed penetration of 20 MVA PV at buses 4 and 5. At this scenario, system loading margin is higher than the concentrated penetration of same rated PV at buses 12 and 14.

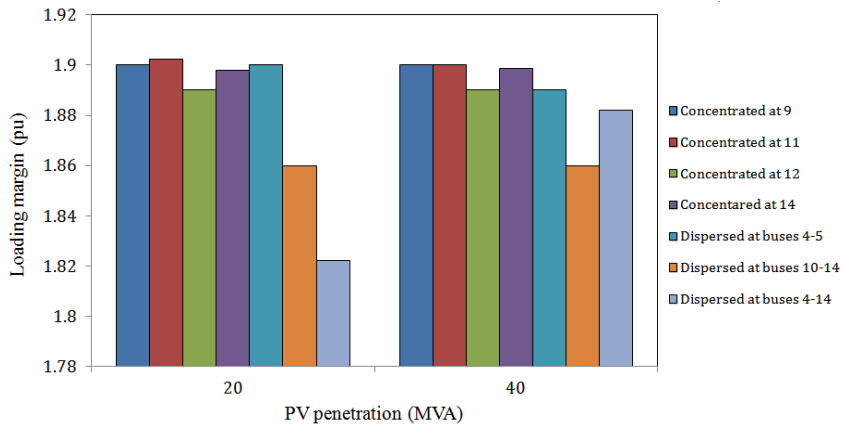


Figure 8. Loading margins for concentrated and dispersed PV penetrations.

C. Location of Dynamic VAr Compensator

For this study PV generators are integrated at buses **12 and 14**, respectively. Three scenarios have been considered to study the effect of dynamic VAr compensator placement on system static voltage stability performance with large-scale PV. These are as follows;

1. Dynamic VAr compensator at each PV generator bus.
2. Dynamic compensator at the weakest bus of the system.
3. Dynamic compensator placed at the bus with highest TSI.

From bus participation factor analysis at stressed condition corresponding to critical eigenvalue reveals that **bus 14** is the weakest bus of the system. Figure 9 displays the trajectory sensitivity index (TSI) of the buses in area-2. TSI is highest for **bus 9**, which is located in the zone where PV generators are integrated to the system. Comparison of system loading margins for STATCOM placements are shown in Figure 10. From Figure 10 it can be seen that system loading margin is highest for TSI based STATCOM placement as compared to STATCOM placement at the weakest bus, and at the point of common coupling of PV generator.

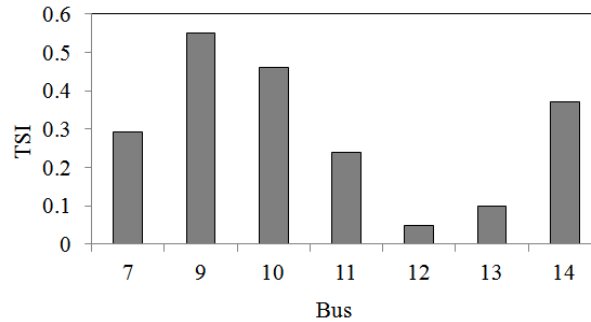


Figure 9. Trajectory sensitivity index values for the buses in area-2.

From results in Figure 10 it can be observed that placement of STATCOM at the weakest bus of the system provides slightly better system loading margin than system without PV, with PV and STATCOM at each PV bus.

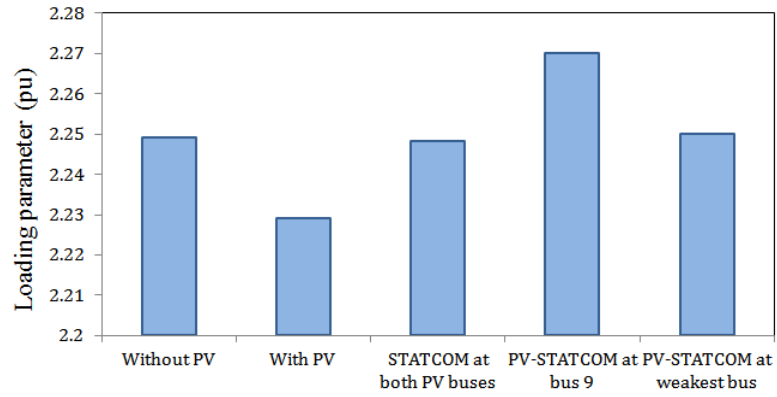


Figure 10. System loading margins for STATCOM placements.

D. Comparison of STATCOM and SVC Performance

Figure 11 shows the comparison of the performance of same MVA rated STATCOM and SVC on power system long-term voltage stability with large-scale PV penetration. The result in Figure 11 shows that STATCOM is more effective in enhancing system static voltage stability margin with large-scale PV integration. However, it is worthwhile to notice that system loading margin is better for SVC placement at each PV generator bus as compared to TSI based placement and the placement at the weakest bus of the system.

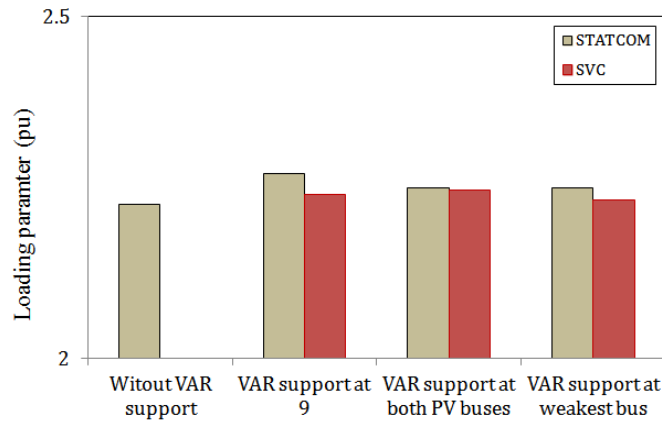


Figure 11. System loading margins for STATCOM and SVC placements.

Conclusions

In this paper, the static voltage stability of the power system with large-scale PV penetration is presented. The main findings of this study are as follows:

- PV location, size and the way they are integrated, i.e., concentrated or dispersed, have profound impact on system static voltage stability.
- Degree of voltage stability deteriorates with the integration of power factor operated PV, whereas, in some cases degree of voltage stability improves with the integration of voltage control mode operated PV.
- The results in this study indicate that the placement of STATCOM based on short term-VAR support to mitigate low voltage ride through problem also provides higher system loading as compared to STATCOM placement at the weakest bus and at PV generator buses.

- STATCOM provides better option to enhance static voltage stability margin of the system with large-scale PVs.
- Placement of SVCs in PV generator buses are found to be more effective in enhancing voltage stability margin rather than the weakest bus placement or the placement based on short term dynamic VAr support.

References

- [1] Photon International, The Solar Power Magazine, April, 2011, [http:// www.photon-magazine.com](http://www.photon-magazine.com).
- [2] M. A. Eltawil and Z. Zhao, "Grid-connected photovoltaic power systems: Technical and potential problems -A review," *Renewable and Sustainable Energy Review*, vol. 14, no. 1, pp. 112-129, 2010.
- [3] Y. T. Tan, D. S. Kirschen, and N. Jenkins, "A model of PV generation suitable for stability analysis," *IEEE Trans. Energy Conversion*, vol. 19, no. 4, pp. 748-755, 2004.
- [4] Y. -B. Wang, C. -S. Wu, H. Liao, and H. -H. Xu, " Study on impacts of large-scale photovoltaic power station on power grid voltage profile," in *Third International Conference on Electric Utility Deregulation, Restructuring and Power Technologies*, 2008.
- [5] X. Xu, Y. Huang, G. He, H. Zhao, and W. Wang, "Modeling of large-scale grid integrated PV station and analysis its impact on grid voltage," in *International Conference on Sustainable Power Generation and supply*, 2009.
- [6] Sode-Yome, N. Mithulananthan, and K. Y. Lee, "Effect of realistic load direction in static voltage stability study," in *IEEE/PES Transmission and Distribution Conference & Exposition: Asia & Pacific*, 2005.
- [7] N. Amjady and M. Esmaili, " Application of new sensitivity analysis framework for voltage contingency ranking," *IEEE Trans. Power Syst.*, vol. 20, no. 2, pp. 973-983, 2005.
- [8] S. Santoso, H. W. Beaty, R. C. Dugan, and M. F. MacGranaghan, "Distributed generation and power quality," in *Electric Power System Quality*, 2nd ed, New York: McGraw-Hill, 2002, pp. 373-435.
- [9] IEEE Application Guide for IEEE Std 1547, IEEE Standard for Interconnecting Distributed Resources with Electric Power Systems, *IEEE Std 1547.2-2008*, pp. 1-207, 2009.
- [10] International Grid Code Comparison (IGCC-list) on line available at http://www.gl-group.com/pdf/IGCC_list.pdf.
- [11] P. Kundur, *Power system stability and control*, *Power System Engineering Series*. New York: McGraw-Hill, 1994.
- [12] K. Clark, N. W. Miller, and R. Walling, "Modeling of GE solar photovoltaic plants for grid studies," General Electric International .Inc, Schenectady, NY 12345, USA, Sep. 9, 2009.
- [13] I. A. Hiskens and M. Akke, "Analysis of the nordel power grid disturbance of using trajectory sensitivities," *IEEE Trans. Power Syst.*, vol. 14, no. 3, pp. 987-994, Aug. 1999.
- [14] I. A. Hiskens and M. A. Pai, "Trajectory sensitivity analysis of hybrid systems," *IEEE Trans. Power Syst.*, vol. 47, no. 2, pp. 204-220, Feb. 2000.
- [15] B. Sapkota and V. Vittal, "Dynamic VAr planning in a large power system using trajectory sensitivities," *IEEE Trans. Power Syst.*, vol. 25, no. 1, pp. 461-469, Feb. 2010.
- [16] M. G. Villalva, J. R. Gazoli, and E. R. Filho, "Comprehensive approach to modeling and simulation of photovoltaic arrays," *IEEE Trans. Power Electronics*, vol. 24, no. 5, pp. 1198-1208, 2009.
- [17] F. Delfino, R. Procopio, R. Rossi, and G. Ronda, "Integration of large-size photovoltaic system in to the distribution grids: a p-q chart approach to assess reactive support capability," *IET Renewable Power Generation*, vol. 4, no. 4, pp.329-340, 2010.

- [18] Sode-Yome, N. Mithulananthan, "Comparison of shunt capacitor, SVC and STATCOM in static voltage stability margin enhancement," *International Journal of Electric Engineering Education*, vol. 41, no. 2, pp. 158-171, April 2004.
- [19] N. G. Hingorani and L. Gyugyi, *Understanding FACTS: concepts and technology of flexible AC transmission systems*, Delhi: IEEE Press, 2001.
- [20] F. Milano, PSAT, MATLAB-based power system analysis toolbox manual, version 2.0, Mar. 2007.
- [21] I. Kamwa, G. Gorndin, and Y. Trudel, "IEEE PSS2B versus PSS4B: The limits of performance of modern power system stabilizers," *IEEE Trans. Power Syst.*, vol. 20, no. 2, pp. 903-915, May 2005.



Rakibuzzaman Shah (S'10) received the B.Sc Eng in EEE from Khulna University of Engineering & Technology (KUET), Khulna, Bangladesh, and the M.Eng from Asian Institute of Technology, Bangkok, Thailand in 2005 and 2009, respectively. He has served as a lecturer at Chittagong University of Engineering & Technology (CUET), Bangladesh for one and half years. Mr. Shah is currently involved in Ph.D. research at University of Queensland, Australia. His main research interests are power system stability, energy security, power system interconnection and renewable

energy technology.



Nadarajah Mithulananathan (SM'10) received his Ph.D from University of Waterloo, Canada in Electrical and Computer Engineering in 2002. Dr. Mithulan is currently a senior lecturer at University of Queensland. He has also served as an associate professor at Asian Institute of Technology, Bangkok, Thailand. His main research interests are voltage stability and oscillation studies on practical power systems, application of FACTS controller and renewable energy technology.



Ramesh Bansal received Ph.D. degree from the Indian Institute of Technology Delhi in 2003. Currently he is a faculty member in the School of Information Technology and Electrical Engineering, The University of Queensland, Australia. His current research interests are in Renewable Energy and Power Systems which includes wind, PV and hybrid systems, AI applications in power systems. Dr. Bansal is an Editor of the IEEE Transactions on Energy Conversion, Associate Editor of the IEEE Transactions on Industrial Electronics and an Editorial Board member of

the IET- Renewable Power Generation, and Electric Power Components and Systems. He is a member of Board of Directors of International Energy Foundation, Alberta, Canada. He is a Senior Member of IEEE.



Kwang Y. Lee (F'01) received his B.S. degree in Electrical Engineering from Seoul National University, Korea, in 1964, M.S. degree in Electrical Engineering from North Dakota State University, Fargo, in 1968, and Ph.D. degree in System Science from Michigan State University, East Lansing, in 1971. He has been on the faculties of Michigan State, Oregon State, Houston, the Pennsylvania State University, and Baylor University, where he is currently Professor and Chair of Electrical and Computer

Engineering and Director of Power and Energy Systems Laboratory. His interests are power systems control, operation and planning, and intelligent systems applications to power plants and power systems control. Dr. Lee is a Fellow of IEEE, Editor of IEEE Transactions on Energy Conversion, and former Associate Editor of IEEE Transactions on Neural Network.



Abraham Lomi (M'2000) received B.Eng and M. Eng degree in electrical engineering from Institute of Technology Nasional, Malang and Institute of Technology Bandung, Indonesia, respectively. He received his PhD (Dr. Eng) degree from Asian Institute of Technology, Thailand. He is currently a full Professor in the Department of Electrical Engineering, Institute of Technology Nasional, Malang, Indonesia. His current research and teaching activities are in the area of Power Electronics, Power Systems, Power Quality and Renewable Energy.